

# Detecting nanohertz gravitational waves with pulsar timing arrays

Xingjiang ZHU<sup>1,2\*</sup>, Linqing WEN<sup>1\*</sup>, George HOBBS<sup>2</sup>, Richard N. MANCHESTER<sup>2</sup> & Ryan M. SHANNON<sup>2,3</sup>

<sup>1</sup>*School of Physics, University of Western Australia, Crawley WA 6009, Australia;*

<sup>2</sup>*CSIRO Astronomy and Space Science, PO Box 76, Epping NSW 1710, Australia;*

<sup>3</sup>*International Centre for Radio Astronomy Research, Curtin University, Bentley, WA 6102, Australia*

Received xxx, 2015; accepted xxx, 2015; published online xxx, 2015

---

Complementary to ground-based laser interferometers, pulsar timing array experiments are being carried out to search for nanohertz gravitational waves. Using the world's most powerful radio telescopes, three major international collaborations have collected ~10-year high precision timing data for tens of millisecond pulsars. In this paper we give an overview on pulsar timing experiments, gravitational wave detection in the nanohertz regime, and recent results obtained by various timing array projects.

**pulsars, gravitational waves, black-hole binaries**

**PACS number(s):** 97.60.Gb, 95.85.Sz, 04.25.dg

---

**Citation:** Zhu X.-J. et al. Detecting nanohertz gravitational waves with pulsar timing arrays. *Sci China-Phys Mech Astron*, 2015, 00: 0000, doi: 0000

---

## 1 Introduction

One hundred years ago, Albert Einstein completed his general theory of relativity, radically revolutionizing our understanding of gravity. In this theory, gravity is no longer a force, but instead an effect of spacetime curvature. The mass and energy content of spacetime creates curvature that in turn dictates the behavior of objects in spacetime. Generally speaking, when a massive object is accelerating, it produces curvature perturbations that propagate at the speed of light. Such *ripples* in the fabric of spacetime are called gravitational waves (GWs).

Forty years ago, Hulse and Taylor discovered the binary-pulsar system PSR B1913+16 [1]. Subsequent observations in the following years showed that its orbital period was gradually decreasing, at a rate that was entirely consistent with that predicted by general relativity as a result of gravitational radiation [2, 3]. This provided the most convincing evidence of the existence of GWs and earned Hulse and Taylor the Nobel prize in Physics in 1993.

It was realized in late 1970s that precision timing observations of pulsars can be used to detect very low frequency GWs ( $\sim 10^{-9}$ – $10^{-7}$  Hz; [4, 5]). Based on a calculation by Estabrook & Wahlquist [6] for the GW detection using Doppler spacecraft tracking, for which the principle is similar to pulsar timing, Detweiler explicitly showed that “*a gravitational wave incident upon either a pulsar or the Earth changes the measured frequency and appears then as a anomalous residual in the pulse arrival time*” [5]. In 1983, Hellings & Downs [7] used timing data from four pulsars to constrain the energy density of any stochastic background to be  $\lesssim 10^{-4}$  times the critical cosmological density at  $\lesssim 10^{-8}$  Hz (see, refs. [8, 9] for similar results). Almost simultaneously to these works, Backer et al. discovered the first millisecond pulsar PSR B1937+21 [10]. Because of its far better rotational stability than any previously known pulsars and relatively narrower pulses, timing observations in the following years improved the limit on stochastic backgrounds very quickly and by orders of magnitude [11–14].

Measurements with a single pulsar can not make definite detections of GWs whose effects may be indistinguishable from other noise processes such as irregular spinning of the

---

\*Corresponding author (Xingjiang ZHU, email: xingjiang.zhu@uwa.edu.au; Linqing WEN, email: linqing.wen@uwa.edu.au)

star itself. By continued timing of an array of millisecond pulsars, i.e., by constructing a pulsar timing array (PTA), GWs can be searched for as correlated signals in the timing data. Hellings & Downs [7] first did such a correlation analysis to put limits on stochastic backgrounds. Romani [15] and Foster & Backer [16] explored the greater scientific potential of PTA experiments: (1) searching for GWs; (2) providing a time standard for long time scales; and (3) detecting errors in the solar system ephemerides.

There are three major PTAs currently operating: the Parkes PTA (PPTA<sup>1</sup>; [17, 18]) was set up in 2004 using the Parkes radio telescope in Australia; the European PTA (EPTA<sup>2</sup>; [19]) was initiated in 2004/2005 and makes use of telescopes in France, Germany, Italy, the Netherlands and the UK; and the North American Nanohertz Observatory for Gravitational Waves (NANOGrav<sup>3</sup>; [20]) was formed in 2007 and carries out observations with the Arecibo and Green Bank telescopes. We summarize in Table 1 information about the telescopes used and the number of pulsars monitored by these PTAs. Recently the three PTA collaborations were combined to form the International PTA (IPTA<sup>4</sup>; [21–23]). Looking into the future, GW detection with pulsar timing observations is one of major science goals for some powerful future radio telescopes, such as the planned Xinjiang Qitai 110 m radio telescope (QTT; which is a fully-steerable single-dish telescope [24]) and the Five-hundred-meter Aperture Spherical Telescope (FAST; which is expected to come online in 2016 [25, 26]) in China, and the planned Square Kilometer Array (SKA) and its pathfinders (see ref. [27] and references therein). Figure 1 shows the distribution of IPTA pulsars on the sky along with those presently known millisecond pulsars that may be useful for PTA research with future telescopes.

**Table 1** Information about pulsar timing array projects.

	<i>Telescope</i>	<i>Diameter</i> (m)	<i>Country</i>	<i>pulsars</i> <sup>a</sup>
PPTA	Parkes	64	Australia	20
	Effelsberg	100	Germany	
	Lovell	76.2	UK	
EPTA	Nancay	94 <sup>b</sup>	France	22
	Sardinia	64	Italy	
	Westerbork	96 <sup>b</sup>	Netherlands	
NANOGrav	Arecibo	305	USA	22
	GBT	100		

*Notes:* <sup>a</sup> We present the number of pulsars that have been timed for more than 5 years for each project here (see table 3 in ref. [22] for more information). It is worth pointing out that a number of pulsars were recently added to the timing arrays and some pulsars were dropped from these arrays. The total number of pulsars that are currently being observed for IPTA is 70, of which 13 are timed by two timing arrays and 10 by all three arrays.

<sup>b</sup> Values of circular-dish equivalent diameter [28].

<sup>1</sup><http://www.atnf.csiro.au/research/pulsar/ppta/>

<sup>2</sup><http://www.epta.eu.org/>

<sup>3</sup><http://nanograv.org/>

<sup>4</sup><http://www.ipta4gw.org/>

<sup>5</sup>See the ATNF Pulsar Catalogue website <http://www.atnf.csiro.au/research/pulsar/psrcat/> for up-to-date information.

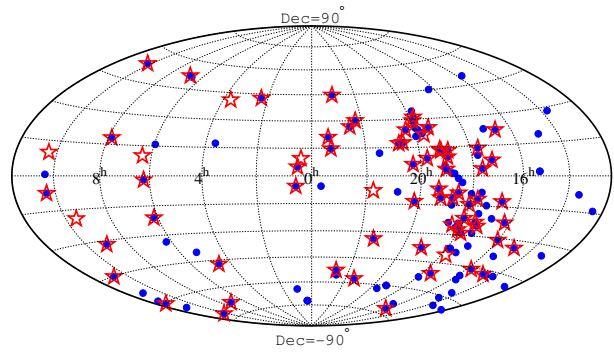


**Figure 1** Distribution of millisecond pulsars on the sky in equatorial coordinates, containing 70 IPTA pulsars (red stars) and all presently known pulsars that have pulse periods  $P < 15$  ms and  $\dot{P} < 10^{-19}$   $\text{ss}^{-1}$  (blue dots; as found in the ATNF Pulsar Catalogue version 1.53 [29])

In this paper, we first introduce the basics of pulsars and pulsar timing techniques in section 2 and 3 respectively. In section 4 we highlight some major noise sources that affect PTA's sensitivities to GWs. In section 5 we describe how a PTA responds to GWs. Section 6 contains a review on GW sources and related results derived from the latest analysis of PTA data. Finally we discuss future prospects in section 7.

## 2 Pulsars

Neutron stars are born as compact remnants of core collapse supernovae during the death of massive main sequence stars with masses of around  $8\text{--}25 M_{\odot}$ . A pulsar is a highly magnetized, spinning neutron star. It can be detected as it emits beams of electromagnetic radiation along its magnetic axis that is misaligned with its rotational axis. Such beams of radiation sweep over the Earth in the same way lighthouse beams sweep across an observer, leading to pulses of radiation received at the observatory. Because of their exceptional rotational stability, pulsars are powerful probes for a wide range of astrophysical phenomena. As mentioned above, long-term timing observations of PSR B1913+16 provided the first observational evidence of the existence of GWs. Timing observations of PSR B1257+12 led to the first confirmed discovery of planets outside our solar system [30]. The double pulsar system PSR J0737–3039A/B, with both neutron stars having been detected as radio pulsars [31, 32], enabled very stringent tests of general relativity and alternative theories of gravity in the strong-field regime [33].

The first pulsar was discovered by Bell and Hewish in 1967 [34]. Since then over 2500 pulsars have been discovered<sup>5</sup>, with spin periods ranging from about 1 millisecond to 10 seconds. It is generally believed that pulsars are born with

periods of order tens of milliseconds but quickly ( $\sim 10$  Myr) spin down (because of the loss of rotational energy) to periods of order seconds. This energy loss could be due to a variety of mechanisms, such as the magnetic dipole radiation, emission of relativistic particle winds and even GWs. As pulsars spin down, they eventually reach a point where there is insufficient energy to power electromagnetic radiation. However, for pulsars in binary systems, it is very likely that pulsars are spun up as mass and angular momentum are accreted from their stellar companions. Such an accretion process is observed in X-ray binaries. These pulsars, usually named as *millisecond pulsars*, have spin periods of about several milliseconds and much lower spin-down rates. Figure 2 shows the distribution of all known pulsars in the period-period derivative diagram.

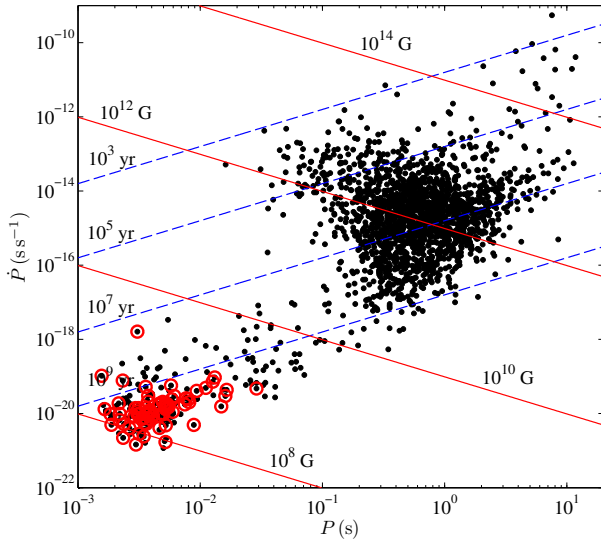


**Figure 2** The period ( $P$ ) vs. period derivative ( $\dot{P}$ ) diagram for all known pulsars (black dots; data taken from the ATNF Pulsar Catalogue version 1.53). Red(grey) circles represent the millisecond pulsars currently being timed by the IPTA project. Also shown are lines of constant characteristic age  $\tau = P/2\dot{P}$  (dash) assuming that pulsars are spinning down solely because of magnetic dipole radiation [35], and of constant inferred surface magnetic field  $B_0 = 3.2 \times 10^{19} \sqrt{P\dot{P}}$  Gauss (solid; [36]). Two distinct populations are apparent in this diagram: (a) *normal pulsars*, with  $P \sim 0.1$ – $4$  seconds and  $B_0 \sim 10^{11}$ – $10^{13}$  Gauss; (b) *millisecond pulsars*, with  $P \sim 3$  milliseconds and  $\dot{P} \sim 10^{-20}$   $\text{ss}^{-1}$ .

### 3 Pulsar timing techniques

Much of the science based on pulsar observations makes use of the “pulsar timing” technique [35, 37, 38], which involves measurement and prediction of pulses’ times of arrival (TOAs). Individual pulses are generally not useful in this regard as they are unstable and mostly too weak to observe. The average pulse profile over a large number of pulses is stable for a particular pulsar at a given observing wavelength, and therefore very suitable for timing experiments.

The first step in pulsar timing is to measure the *topocentric* pulse arrival times with clocks local to the radio observatories. Data collected with the telescope are *de-dispersed*

to correct for frequency-dependent dispersion delays due to the ionized interstellar medium. These data are then *folded* with the period derived from previous observations to form the mean pulse profile. This profile is then correlated with a standard template, either an analytic function or simply a very high signal-to-noise ratio observation, to record the pulse arrival time at the observatory.

The measured TOAs are further transformed to the pulse emission time via a *timing model*, from which the pulse phase of emission is computed. The rotational phase  $\phi(t)$  of the pulsar as a function of time  $t$  (measured in an inertial reference frame of the pulsar) can be represented as a Taylor series:

$$\phi(t) = \phi(t_0) + f(t - t_0) + \frac{1}{2}\dot{f}(t - t_0)^2 + \dots, \quad (1)$$

where  $t_0$  is an arbitrary reference time,  $f = d\phi/dt$  is the spin frequency, and  $\dot{f}$  is the frequency derivative. A number of corrections are applied when converting the topocentric TOAs to the pulsar frame. Such corrections include:

1. Clock corrections, which account for differences in the observatory time and a realization of Terrestrial Time (e.g., the International Atomic Time).
2. pulse delay induced by Earth’s troposphere.
3. the Einstein delay, i.e., the time dilation due to changes in the gravitational potential of the Earth, the Earth’s motion, and the secular motion of the pulsar or that of its binary system.
4. the Roemer delay, i.e., the vacuum light travel time between the observatory and the solar system barycenter, and for pulsars in binaries between the pulsar and the binary system’s barycenter.
5. Shapiro delays, i.e., gravitational time delays due to the solar system objects and if applicable the pulsar’s companion.
6. Dispersion delays caused by the interstellar medium, the interplanetary medium and the Earth’s ionosphere.

The timing model, which describes the above corrections and the pulsar’s intrinsic rotational behavior, predicts the rotational phase of the pulsar at any given time as observed from the solar system barycenter. Basic parameters of a pulsar timing model include the spin period, spin-down rate, right ascension and declination of the pulsar, the dispersion measure (discussed later in section 4), and Keplerian orbital parameters if the pulsar is in a binary system. Measured TOAs are compared with predictions based on the timing model, and the differences are called *timing residuals*. The (pre-fit) timing residual for the  $i$ -th observation is calculated as [39]:

$$R_i = \frac{\phi(t_i) - N_i}{f}, \quad (2)$$

where  $N_i$  is the nearest integer<sup>6</sup> to each  $\phi(t_i)$ . One can see the key point in pulsar timing is that every single rotation of the pulsar is unambiguously accounted for over long periods (years to decades) of time.

A linear least-squares fitting procedure is carried out to obtain estimates of timing parameters, their uncertainties and the post-fit timing residuals. In practice, this is done iteratively: one starts from a small set of data and only includes the most basic parameters (with values derived from previous observations) so that it is easier to coherently track the rotational phase. Parameter estimates are then improved by minimizing the timing residuals and additional parameters can be included for a longer data set.

The fitting to a timing model and analysis of the timing residuals can be performed with the pulsar timing software package TEMPO2 [37, 39, 40], which is freely available on the internet for download<sup>7</sup>. More recently, an alternative method based on Bayesian inference was also developed [41, 42].

#### 4 Noise sources in pulsar timing data

Timing residuals generally come from two groups of contribution: (1) un-modelled deterministic processes, e.g., an unknown binary companion or a single-source GW; and (2) stochastic processes, e.g., the intrinsic pulsar spin noise and a GW background. Before the discussion of GW detection with PTAs, we briefly discuss some major noise processes in pulsar timing data here.

##### Radiometer noise

Radiometer noise arises from the observing system and the radio sky background (including the atmosphere, the cosmic microwave background and synchrotron emission in the Galactic plane). It can be quantified as [35]:

$$\sigma_{\text{rad.}} \approx \frac{W}{S/N} \approx \frac{WS_{\text{sys}}}{S_{\text{mean}} \sqrt{2\Delta\nu t_{\text{int}}}} \sqrt{\frac{W}{P-W}}, \quad (3)$$

where  $W$  and  $P$  are the pulse width and period respectively,  $S/N$  is the profile signal-to-noise ratio,  $S_{\text{sys}}$  is the system equivalent flux density which depends on the system temperature and the telescope's effective collecting area,  $S_{\text{mean}}$  the pulsar's flux density averaged over its pulse period,  $\Delta\nu$  and  $t_{\text{int}}$  are the observation bandwidth and integration time respectively. Radiometer noise can be reduced by using low-noise receivers, observing with larger telescopes, and increasing observing time and bandwidth. One reason to fold individual pulses to obtain an average profile is to reduce the radiometer noise; the reduction is equal to the square root of the number of pulses folded. Radiometer noise is an additive Gaussian white noise and is formally responsible for TOA uncertainties. From equation (3), one can see that bright, fast

spinning pulsars with narrow pulse profiles allow the highest timing precision.

##### Pulse jitter noise

Pulse jitter manifests as the variability in the shape and arrival phase of individual pulses. The mean pulse profile is an average over a large number of single pulses. Although it is stable for most practical purposes, there always exists some degree of stochasticity in the phase and amplitude of the average pulse profile. Pulse jitter noise is intrinsic to the pulsar itself, and thus can only be reduced by increasing observing time, i.e., averaging over more single pulses. Pulse jitter is also a source of white noise, which has been found to be a limiting factor of the timing precision for a few very bright pulsars [43, 44]. For future telescopes such as FAST and SKA, jitter noise may dominate over the radiometer noise for many millisecond pulsars [26]. Improvement in the timing precision for the brightest pulsar PSR J0437-4715 was recently demonstrated with the use of some mitigation methods for pulse jitter noise [45, 46].

##### “Timing noise”

It has long been realized that timing residuals of many pulsars show structures that are inconsistent with TOA uncertainties [47, 48]. Such structures are collectively referred to as *timing noise*. Timing noise is very commonly seen in normal pulsars and has also become more prominent in a number of millisecond pulsars as timing precision increases and the data span grows. The exact astrophysical origins of timing noise are not well understood. It is mostly suggested to be related to rotational irregularities of the pulsar and therefore it is also usually called as spin noise [49, 50]. For millisecond pulsars, power spectra of timing residuals can typically be modelled as the sum of white noise and red noise. For red noise, a power law spectrum with a low-frequency turnover appears to be a good approximation (see, e.g., figure 11 in ref. [17] for analyses of 20 PPTA pulsars).

The presence of red noise results in problems to the pulsar timing analysis as the standard least-squares fitting of a timing model assumes time-independent TOA errors. Blandford et al. [47] analytically showed the effects of timing noise on the estimates of timing model parameters and suggested the use of the noise covariance matrix to pre-whiten the data for improved parameter estimation. More recently, Coles et al. [51] developed a whitening method that uses the Cholesky decomposition of the covariance matrix of timing residuals to whiten both the residuals and the timing model. By doing so, noise in the whitened residuals is statistically white and the ordinary least-squares solution of a timing model can be obtained. van Haasteren & Levin [52] developed a Bayesian

<sup>6</sup>Here note that  $\phi(t)$  is measured in *turns* equal to  $2\pi$  radians.

<sup>7</sup>[www.sf.net/projects/tempo2/](http://www.sf.net/projects/tempo2/)



framework that is capable of simultaneously estimating timing model parameters and timing noise spectra.

### Dispersion measure variations

Because of dispersion due to the interstellar plasma, pulses at low frequencies arrive later than at high frequencies. Specifically, this dispersion delay is given by:

$$\Delta_{\text{DM}} \approx (4.15 \text{ ms}) \text{DM} \nu_{\text{GHz}}^{-2}, \quad (4)$$

where  $\nu_{\text{GHz}}$  is the radio frequency measured in GHz, and dispersion measure (DM, measured in  $\text{pc cm}^{-3}$ ) is the integrated column density of free electrons between an observer and a pulsar. Because of the motion of the Earth and the pulsar relative to the interstellar medium, the DM of a pulsar is not a constant in time. Such DM variations introduce time-correlated noise in pulsar timing data.

Pulsars in a timing array are usually observed quasi-simultaneously at two or more different frequencies. For example, the PPTA team observes pulsars at three frequency bands – 50 cm ( $\sim 700$  MHz), 20 cm ( $\sim 1400$  MHz), and 10 cm ( $\sim 3100$  MHz) – during each observing session (typically 2-3 days). This makes it possible to account for DM variations and thus reduce the associated noise with various methods [53–55]. The method currently being used by the PPTA is described in Keith et al. [54], which was built on a previous work by You et al. [56]. In this method timing residuals are modelled as the combination of a (radio-)wavelength-independent (i.e., common-mode) delay and the dispersion delay. Both components are represented as piece-wise linear functions and can be estimated through a standard least-squares fit. A key feature of this method is that GW signals are preserved in the common-mode component. Ultra wide-band receivers are in development by various collaborations in order to better correct for noise induced by DM variations (along with other benefits such as increasing timing precision, studies of interstellar medium, and etc.).

### Interstellar scintillation

Interstellar scintillation refers to strong scattering of radio waves due to the spatial inhomogeneities in the ionized interstellar medium [57], analogous to twinkling of stars due to scattering in the Earth's atmosphere. There are multiple effects associated with interstellar scintillation that cause time-varying delays in measured TOAs, with the dominant one being pulse broadening from multipath scattering [58, 59]. Various mitigation techniques have been developed for this type of noise [59–61]. Generally speaking, noise induced by interstellar scintillation is a Gaussian white noise, and can be reduced by increasing observing time and bandwidth. For millisecond pulsars that are observed at current radio frequencies by PTAs, the effects of scintillation are predicted to

be small. However, when pulsars are observed at lower frequencies, or more distant (and more scintillated) pulsars are observed, these effects can become more important [59, 62].

### Correlated noise among different pulsars

The above noise processes are generally thought to be uncorrelated among different pulsars. In a PTA data set that we hope to detect GWs, some correlated noise may be present. For example, (1) instabilities in Terrestrial Time standards affect TOA measurements of all pulsars in exactly the same way, i.e., clock errors result in a *monopole* signature in a PTA data set; (2) the solar system ephemerides, which provide accurate predictions of the masses and positions of all the major solar system objects as a function of time, are used to convert pulse arrival times at the observatory to TOAs referenced at the solar system barycenter. Imperfections in the solar system ephemerides induce a *dipole* correlation in a PTA data set. Indeed, it has been demonstrated that PTAs can be used (1) to search for irregularities in the time standard and thus to establish a pulsar-based timescale [63], and (2) to measure the mass of solar system planets [64].

## 5 Gravitational waves and pulsar timing arrays

The effects of GWs in a single-pulsar data may be indistinguishable from those due to noise processes as discussed in the previous subsection. Indeed, even without any such noise, GWs that have the same features as those due to uncertainties in the timing model parameters would still be very difficult to detect with only one pulsar. Therefore analysis of single-pulsar data can be best used to constrain the strength of potential GWs [65, 66].

A PTA is a Galactic-scale GW detector. If one wishes to have an analogy to a laser interferometer, pulsars in the timing array are “test masses”; pulses of radio waves act as the laser; and the pulsar-Earth baseline is a single “arm”. Millisecond pulsars in our Galaxy, typically  $\sim \text{kpc}$  (or thousands of light years) away, emit radio waves that are received at the telescope with extraordinary stability. A GW passing across the pulsar-Earth baseline perturbs the local spacetime along the path of radio wave propagation, leading to an apparent redshift in the pulse frequency that is proportional to the GW strain amplitude. Let us first consider the special case where a linearly polarized GW propagates in a direction perpendicular to the pulsar-Earth baseline, the resulting timing residual is given by:

$$r(t) = \int_0^{L/c} h(t - \frac{L}{c} + \tau) d\tau, \quad (5)$$

where  $L$  is the pulsar distance and we adopt the plane wave approximation<sup>8</sup>. With the definition of  $dA(t)/dt = h(t)$ , the

<sup>8</sup>For sources that are close enough ( $\leq 100$  Mpc), it may be necessary to consider the curvature of the gravitational wavefront. This, in principle, would allow luminosity distances to GW sources to be measured via a parallax effect [67].

timing residual takes the following form:

$$r(t) = \Delta A(t) = A(t) - A\left(t - \frac{L}{c}\right). \quad (6)$$

Here we can see that  $A(t)$  results from the GW induced space-time perturbation incident on the Earth (i.e., the *Earth term*), and  $A\left(t - \frac{L}{c}\right)$  depends on the GW strain at the time of the radio wave emission (i.e., the *pulsar term*). Typical PTA observations have a sampling interval of weeks and span over  $\sim 10$  yr, implying a sensitive frequency range of  $\sim 1$ – $100$  nHz. Therefore PTAs are sensitive to GWs with wavelengths of several light years, much smaller than the pulsar-Earth distance.

In the general case where a GW originates from a direction  $\hat{\Omega}$ , the induced timing residuals can be written as:

$$r(t, \hat{\Omega}) = F_+(\hat{\Omega})\Delta A_+(t) + F_\times(\hat{\Omega})\Delta A_\times(t), \quad (7)$$

where  $F_+(\hat{\Omega})$  and  $F_\times(\hat{\Omega})$  are antenna pattern functions as given by [68]:

$$F_+(\hat{\Omega}) = \frac{1}{4(1 - \cos\theta)} \left\{ (1 + \sin^2\delta) \cos^2\delta_p \cos[2(\alpha - \alpha_p)] - \sin 2\delta \sin 2\delta_p \cos(\alpha - \alpha_p) + \cos^2\delta (2 - 3\cos^2\delta_p) \right\} \quad (8)$$

$$F_\times(\hat{\Omega}) = \frac{1}{2(1 - \cos\theta)} \left\{ \cos\delta \sin 2\delta_p \sin(\alpha - \alpha_p) - \sin\delta \cos^2\delta_p \sin[2(\alpha - \alpha_p)] \right\}, \quad (9)$$

where  $\cos\theta = \cos\delta \cos\delta_p \cos(\alpha - \alpha_p) + \sin\delta \sin\delta_p$ ,  $\theta$  is the opening angle between the GW source and pulsar with respect to the observer, and  $\alpha$  ( $\alpha_p$ ) and  $\delta$  ( $\delta_p$ ) are the right ascension and declination of the GW source (pulsar) respectively. The source-dependent functions  $\Delta A_{+, \times}(t)$  in equation (7) are given by:

$$\Delta A_{+, \times}(t) = A_{+, \times}(t) - A_{+, \times}(t_p) \quad (10)$$

$$t_p = t - (1 - \cos\theta) \frac{L}{c}. \quad (11)$$

The forms of  $A_+(t)$  and  $A_\times(t)$  depend on the type of source that we are looking for.

### The Hellings-Downs curve

An isotropic stochastic background will produce a correlated signal in PTA data sets. Such a correlation uniquely depends on the angular separation between pairs of pulsars, as given by [7]:

$$\zeta(\theta_{ij}) = \frac{3}{2} \frac{(1 - \cos\theta_{ij})}{2} \ln \left[ \frac{(1 - \cos\theta_{ij})}{2} \right] - \frac{1}{4} \frac{(1 - \cos\theta_{ij})}{2} + \frac{(1 + \delta_{ij})}{2}, \quad (12)$$

where  $\theta_{ij}$  is the angle between pulsars  $i$  and  $j$ , and  $\delta_{ij}$  is 1 for  $i = j$  and 0 otherwise. Figure 3 shows the famous Hellings-Downs curve as given by equation (12) – it is a factor of  $3/2$

larger than the original result of ref. [7]. This is because  $\zeta(\theta_{ij})$  is normalized to 1 for the autocorrelation of the stochastic background induced timing residuals for a single pulsar. In Figure 3 the correlation function takes a value of 0.5 at zero angular separation as the autocorrelation due to pulsar terms is neglected.

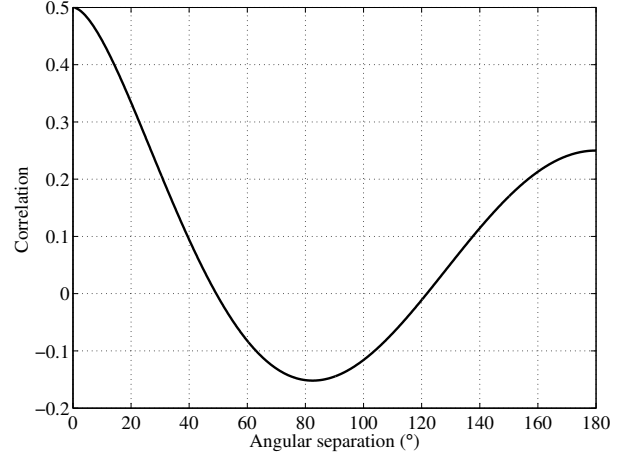


**Figure 3** The Hellings-Downs curve, which depicts the expected correlation in timing residuals due to an isotropic stochastic background, as a function of the angular separation between pairs of pulsars.

## 6 Gravitational wave sources and recent observational results

Potential signals that could be detectable for PTAs include: (1) stochastic backgrounds. The primary target is that formed by the combined emission from numerous binary supermassive black holes distributed throughout the Universe. Background signals from cosmic strings (e.g., [69]) and inflation (e.g., [70, 71]) have also been studied in the context of PTAs; (2) continuous waves, which can be produced by individual nearby binaries; (3) bursts with memory associated with binary black hole mergers; (4) and all other GW bursts. Below we give a brief overview of these sources and summarize some recent astrophysical results.

### Stochastic backgrounds

The stochastic background from the cosmic population of supermassive binary black holes has been the most popular target for PTA efforts. Generally speaking the signal amplitude depends on how frequently these binaries merge in cosmic history and how massive they are. Both of these quantities are poorly constrained observationally. Assuming that all binaries are in circular orbits and evolve through gravitational radiation only, the characteristic amplitude spectrum of this background is given by [72–78]:

$$h_c(f) = A_{\text{yr}} \left( \frac{f}{f_{\text{yr}}} \right)^{-2/3}, \quad (13)$$

where  $A_{\text{yr}}$  is the dimensionless amplitude at a reference frequency  $f_{\text{yr}} = 1 \text{ yr}^{-1}$ . The fraction of the cosmological critical energy density (per logarithmic frequency interval) contained in the GW background is related to the amplitude spectrum through  $\Omega_{\text{GW}}(f) = (2\pi^2/3H_0^2)A_{\text{yr}}^2 f_{\text{yr}}^2 (f/f_{\text{yr}})^{2/3}$  where  $H_0$  is the Hubble constant. Various models predict a similar range of  $A_{\text{yr}}$ , most likely to be  $\sim 10^{-15}$  (see, e.g., [75–77]). An exception is the recent model in ref. [78] whose prediction is two to five times higher. Recent studies that include the effects of environmental coupling and orbital eccentricities indicate a reduced signal at below  $\sim 10 \text{ nHz}$  [79–81].

Jenet et al. [82] suggested that it is possible to make a detection of the binary black hole background if 20 pulsars are timed with a precision of  $\sim 100 \text{ ns}$  over  $\geq 5$  years. Three PTAs have searched for such a background signal assuming it is isotropic, leading to increasingly more stringent upper limits on the background strength [53, 83–87]. The most constraining limit published to date ( $A_{\text{yr}} < 2.4 \times 10^{-15}$ ) comes from the PPTA collaboration by Shannon et al. [87]. As shown in Figure 4, this limit ruled out the most optimistic model of [78] with 90% confidence and is in tension with other models at  $\sim 50\%$  confidence.

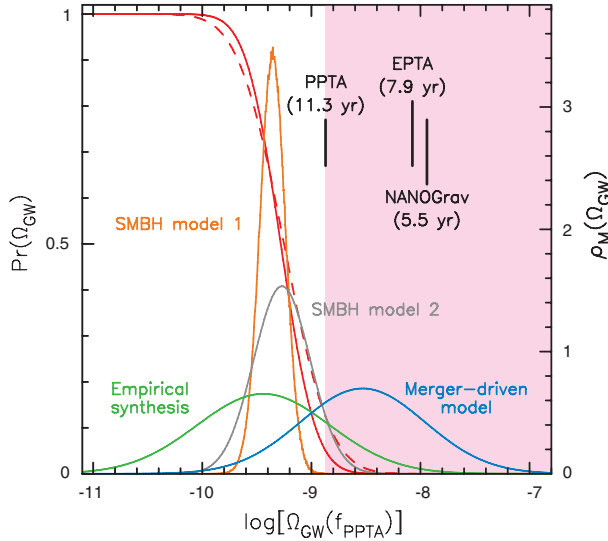


**Figure 4** Upper limits on the fractional energy density of the GW background  $\Omega_{\text{GW}}(f)$ , at a frequency of 2.8 nHz, as compared against various models of the supermassive binary black hole background. The red(grey) solid and dashed lines show the probabilities  $\text{Pr}(\Omega_{\text{GW}})$  that a GW background with energy density  $\Omega_{\text{GW}}(f)$  exists given the PPTA data, assuming Gaussian and non-Gaussian statistics respectively. Three vertical lines mark the 95% confidence upper limits published by NANOGrav [53], EPTA [85] and PPTA [87], where the times next to these lines correspond approximately to the observing spans of the data sets. The shaded region is ruled out with 95% confidence by the PPTA data. Gaussian curves represent the probability density functions  $\rho_M(\Omega_{\text{GW}})$  given different models: a merger-driven model for growth of massive black holes in galaxies [78], a synthesis of empirical models [76], semi-analytic models (SMBH model 1; [87]) based on the Millennium dark matter simulations [88, 89] and a distinct model for black hole growth (SMBH model 2; [90]). Figure taken from ref. [87].

<sup>9</sup>More recently, the EPTA group obtained slightly better limits for  $f < 10 \text{ nHz}$  and comparable results at higher frequencies [113].

Recently methods have also been proposed to search for a more general anisotropic background signal [91–94]. Using the 2015 EPTA data, Taylor et al. [95] placed constraints on the angular power spectrum of the background from circular, GW-driven supermassive black hole binaries and found that the data could not update the prior knowledge on the angular distribution of a GW background.

## Continuous waves

Individual supermassive binary black holes, especially the most nearby and/or massive ones, could provide good opportunities for detection of continuous waves. Unlike compact binaries in the audio band, supermassive binary black holes detectable for PTAs are mostly in the early stage of inspiral and therefore emit quasi-monochromatic waves. For an inspiralling circular binary of component masses  $m_1$  and  $m_2$ , the GW strain amplitude is given by [96]:

$$h_0 = 2 \frac{(GM_c)^{5/3} (\pi f)^{2/3}}{c^4 d_L}, \quad (14)$$

where  $d_L$  is the luminosity distance of the source, and  $M_c$  is the chirp mass defined as  $M_c = M\eta^{5/3}$ , with  $M = m_1 + m_2$  the total mass and  $\eta = m_1 m_2 / M^2$  the symmetric mass ratio. After averaging over the antenna pattern functions given by equations (8-9) and the binary orbital inclination angle, the Earth-term timing residuals induced by a circular binary is  $\sim h_0 / 2\pi f$ .

Before the establishment of major PTAs, Jenet et al. [65] developed a framework in which pulsar timing observations can be used to constrain properties of supermassive binary black holes and applied the method to effectively rule out the claimed binary black hole system in 3C 66B [97]. In recent years growing efforts have gone into investigating the detection prospects [98–102] of, and designing data analysis methods [103–109] for, continuous waves.

Yardley et al. [110] calculated the first sensitivity curve of a PTA to this type of sources using an earlier PPTA data set presented in ref. [111]. Recently both PPTA [108] and NANOGrav [112] conducted searches for continuous waves in their corresponding real data sets. Because of its excellent data quality, PPTA has achieved by far the best sensitivity for continuous waves. Figure 5 shows a sky map of PPTA's sensitivities to circular binary black holes of chirp mass  $10^9 M_\odot$  and orbital period of  $\sim 6$  years [108]. Unfortunately most nearby galaxy clusters or binary black hole candidates are within the less sensitive sky region. Zhu et al. [108] also presented very stringent upper limit<sup>9</sup> on the GW strain amplitude ( $h_0 < 1.7 \times 10^{-14}$  at 10 nHz) and on the local merger rate density of supermassive binary black holes (fewer than  $4 \times 10^{-3} \text{ Mpc}^{-3} \text{ Gyr}^{-1}$  for  $M_c \geq 10^{10} M_\odot$ ).

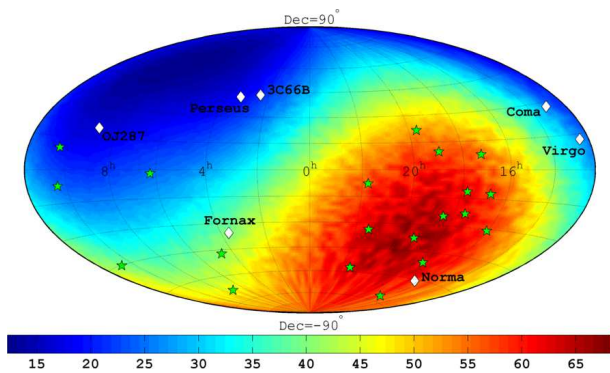


**Figure 5** Sky distribution of luminosity distance (in Mpc) out to which a circular binary black hole of chirp mass  $10^9 M_\odot$  and orbital period of 5 nHz could be detected with the PPTA data set. Sky locations of the 20 PPTA pulsars are indicated by “★”. White diamonds mark the location of possible supermassive black hole binary candidates or nearby clusters: Virgo (16.5 Mpc), Fornax (19 Mpc), Norma (67.8 Mpc), Perseus (73.6 Mpc), 3C 66B (92 Mpc), Coma (102 Mpc) and OJ287 (1.07 Gpc). Figure originally published in ref. [108].

### Gravitational wave memory

A GW memory is a permanent distortion in the spacetime metric [114, 115]. Such effects can be produced during mergers of supermassive binary black holes and cause instantaneous jumps of pulse frequency. For a single pulsar, this is indistinguishable from a glitch event. With a timing array, GW memory effects can be searched for as simultaneous pulse frequency jumps in all pulsars when the burst reaches the Earth. It has been suggested that GW memory signals are in principle detectable with current PTAs for black hole mass of  $10^8 M_\odot$  within a redshift of 0.1 [116–119]. However, the event rate is highly uncertain. Current estimates are very pessimistic, predicting only 0.03 to 0.2 detectable events every 10 years for future PTA observations based on the SKA [101, 120]. Actual searches in existing PTA data sets – see ref. [121] for PPTA and ref. [122] for NANOGrav – have set upper limits on the memory event rate, which remain orders of magnitude above theoretical expectations.

### Gravitational wave bursts

Potential burst sources of interest to PTAs include the formation or coalescence of supermassive black holes, the periastron passage of compact objects in highly elliptic or unbound orbits around a supermassive black hole [123], cosmic (super)string cusps and kinks [124–126], and triplets of supermassive black holes [127]. Finn & Lommen [123] developed a Bayesian framework for detecting and characterizing burst GWs (see also ref. [128]). Zhu et al. [109] recently proposed a general coherent (frequentist) method that can be used to search for GW bursts with PTAs. No specific predictions have been made for detecting GW bursts with PTAs in the literature. There has been no published results on searches for bursts using real PTA data.

## 7 Summary and future prospects

With their existence predicted by general relativity one century ago, GWs have not yet been directly detected. However, it is widely believed that we are on the threshold of opening the gravitational window into the Universe. In the audio band (from 10 to several kHz), 2nd-generation laser interferometers such as Advanced LIGO are about to start scientific observations and a detection of signals from compact binary coalescences (e.g., binary neutron star inspirals) is likely within a few years (see the article by Reitze et al. in this issue). In the nanohertz frequency range, PTA experiments have achieved unprecedented sensitivities and started to put serious constraints on the cosmic population of supermassive black hole binaries.

The sensitivity of a PTA can be improved by a) increasing the data span and observing cadence, b) including more pulsars in the array, and c) reducing the noise present in the data. Regarding the first two factors, the combination of data sets from three PTAs to a single IPTA data set offers the most straightforward benefit. Other ongoing efforts include optimization of observing strategies, searches for millisecond pulsars, characterization of various noise processes and corresponding mitigation methods, and development of advanced instrumentations. In the longer term, pulsar timing observations with FAST and SKA will provide advances in all aspects of PTA science, not only leading to the detection of GWs but also allowing detailed studies of the nanohertz gravitational Universe.

XZ, LW and GH acknowledge funding support from the Australian Research Council.

- 1 R. A. Hulse and J. H. Taylor. Discovery of a pulsar in a binary system. *ApJ*, 195:L51–L53, 1975.
- 2 J. H. Taylor and J. M. Weisberg. A new test of general relativity - Gravitational radiation and the binary pulsar PSR 1913+16. *ApJ*, 253:908–920, 1982.
- 3 J. M. Weisberg, D. J. Nice, and J. H. Taylor. Timing Measurements of the Relativistic Binary Pulsar PSR B1913+16. *ApJ*, 722:1030–1034, 2010.
- 4 M. V. Sazhin. Opportunities for detecting ultralong gravitational waves. *Soviet Astronomy*, 22:36–38, 1978.
- 5 S. Detweiler. Pulsar timing measurements and the search for gravitational waves. *ApJ*, 234:1100–1104, 1979.
- 6 F. B. Estabrook and H. D. Wahlquist. Response of Doppler spacecraft tracking to gravitational radiation. *General Relativity and Gravitation*, 6:439–447, 1975.
- 7 R. W. Hellings and G. S. Downs. Upper limits on the isotropic gravitational radiation background from pulsar timing analysis. *ApJ*, 265:L39–L42, 1983.
- 8 R. W. Romani and J. H. Taylor. An upper limit on the stochastic background of ultralow-frequency gravitational waves. *ApJ*, 265:L35–L37, 1983.
- 9 B. Bertotti, B. J. Carr, and M. J. Rees. Limits from the timing of pulsars on the cosmic gravitational wave background. *MNRAS*, 203:945–954, 1983.



- 10 D. C. Backer, S. R. Kulkarni, C. Heiles, et al. A millisecond pulsar. *Nature*, 300:615–618, 1982.
- 11 M. M. Davis, J. H. Taylor, J. M. Weisberg, et al. High-precision timing observations of the millisecond pulsar PSR 1937 + 21. *Nature*, 315:547–550, 1985.
- 12 L. A. Rawley, J. H. Taylor, M. M. Davis, et al. Millisecond pulsar PSR 1937+21 - A highly stable clock. *Science*, 238:761–765, 1987.
- 13 D. R. Stinebring, M. F. Ryba, J. H. Taylor, et al. Cosmic gravitational-wave background - Limits from millisecond pulsar timing. *Physical Review Letters*, 65:285–288, 1990.
- 14 V. M. Kaspi, J. H. Taylor, and M. F. Ryba. High-precision timing of millisecond pulsars. 3: Long-term monitoring of PSRs B1855+09 and B1937+21. *ApJ*, 428:713–728, 1994.
- 15 R. W. Romani. Timing a millisecond pulsar array. In H. Ögelman and E. P. J. van den Heuvel, editors, *NATO Advanced Science Institutes (ASI) Series C*, volume 262, page 113, 1989.
- 16 R. S. Foster and D. C. Backer. Constructing a pulsar timing array. *ApJ*, 361:300–308, 1990.
- 17 R. N. Manchester, G. Hobbs, M. Bailes, et al. The Parkes Pulsar Timing Array Project. *PASA*, 30:17, 2013.
- 18 G. Hobbs. The Parkes Pulsar Timing Array. *Class. Quantum Gravity*, 30(22):224007, 2013.
- 19 M. Kramer and D. J. Champion. The European Pulsar Timing Array and the Large European Array for Pulsars. *Class. Quantum Gravity*, 30(22):224009, 2013.
- 20 M. A. McLaughlin. The North American Nanohertz Observatory for Gravitational Waves. *Class. Quantum Gravity*, 30(22):224008, 2013.
- 21 G. Hobbs, A. Archibald, Z. Arzumianian, et al. The International Pulsar Timing Array project: using pulsars as a gravitational wave detector. *Class. Quantum Gravity*, 27(8):084013, 2010.
- 22 R. N. Manchester. The International Pulsar Timing Array. *Class. Quantum Gravity*, 30(22):224010, 2013.
- 23 M. A. McLaughlin. The International Pulsar Timing Array: A Galactic Scale Gravitational Wave Observatory. *arXiv:1409.4579v2*, 2014.
- 24 N. Wang. Xinjiang Qitai 110 m radio telescope (in Chinese). *Sci China-Phys Mech Astron*, 44:783–794, 2014.
- 25 R. Nan, D. Li, C. Jin, et al. The Five-Hundred Aperture Spherical Radio Telescope (fast) Project. *International Journal of Modern Physics D*, 20:989–1024, 2011.
- 26 G. Hobbs, S. Dai, R. N. Manchester, et al. The Role of FAST in Pulsar Timing Arrays. *arXiv:1407.0435v1*, 2014.
- 27 T. J. W. Lazio. The Square Kilometre Array pulsar timing array. *Class. Quantum Gravity*, 30(22):224011, 2013.
- 28 R. D. Ferdman, R. van Haasteren, C. G. Bassa, et al. The European Pulsar Timing Array: current efforts and a LEAP toward the future. *Class. Quantum Gravity*, 27(8):084014, 2010.
- 29 R. N. Manchester, G. B. Hobbs, A. Teoh, et al. The Australia Telescope National Facility Pulsar Catalogue. *AJ*, 129:1993–2006, 2005.
- 30 A. Wolszczan and D. A. Frail. A planetary system around the millisecond pulsar PSR1257 + 12. *Nature*, 355:145–147, 1992.
- 31 M. Burgay, N. D’Amico, A. Possenti, et al. An increased estimate of the merger rate of double neutron stars from observations of a highly relativistic system. *Nature*, 426:531–533, 2003.
- 32 A. G. Lyne, M. Burgay, M. Kramer, et al. A Double-Pulsar System: A Rare Laboratory for Relativistic Gravity and Plasma Physics. *Science*, 303:1153–1157, 2004.
- 33 M. Kramer, I. H. Stairs, R. N. Manchester, et al. Tests of General Relativity from Timing the Double Pulsar. *Science*, 314:97–102, 2006.
- 34 A. Hewish, S. J. Bell, J. D. H. Pilkington, et al. Observation of a Rapidly Pulsating Radio Source. *Nature*, 217:709–713, 1968.
- 35 D. R. Lorimer and M. Kramer. *Handbook of pulsar astronomy*. Cambridge Uni. Press, Cambridge, 2005.
- 36 R. N. Manchester and J. H. Taylor. *Pulsars*. WH Freeman and Company, San Francisco, 1977.
- 37 R. T. Edwards, G. B. Hobbs, and R. N. Manchester. TEMPO2, a new pulsar timing package - II. The timing model and precision estimates. *MNRAS*, 372:1549–1574, 2006.
- 38 A. N. Lommen and P. Demorest. Pulsar timing techniques. *Class. Quantum Gravity*, 30(22):224001, 2013.
- 39 G. B. Hobbs, R. T. Edwards, and R. N. Manchester. TEMPO2, a new pulsar-timing package - I. An overview. *MNRAS*, 369:655–672, 2006.
- 40 G. Hobbs, F. Jenet, K. J. Lee, et al. TEMPO2: a new pulsar timing package - III. Gravitational wave simulation. *MNRAS*, 394:1945–1955, 2009.
- 41 L. Lentati, P. Alexander, M. P. Hobson, et al. TEMPONEST: a Bayesian approach to pulsar timing analysis. *MNRAS*, 437:3004–3023, 2014.
- 42 S. J. Vigeland and M. Vallisneri. Bayesian inference for pulsar-timing models. *MNRAS*, 440:1446–1457, 2014.
- 43 R. M. Shannon, S. Osłowski, S. Dai, et al. Limitations in timing precision due to single-pulse shape variability in millisecond pulsars. *MNRAS*, 443:1463–1481, 2014.
- 44 T. Dolch, M. T. Lam, J. Cordes, et al. A 24 Hr Global Campaign to Assess Precision Timing of the Millisecond Pulsar J1713+0747. *ApJ*, 794:21, 2014.
- 45 S. Osłowski, W. van Straten, G. B. Hobbs, et al. High signal-to-noise ratio observations and the ultimate limits of precision pulsar timing. *MNRAS*, 418:1258–1271, 2011.
- 46 S. Osłowski, W. van Straten, P. Demorest, et al. Improving the precision of pulsar timing through polarization statistics. *MNRAS*, 430:416–424, 2013.
- 47 R. Blandford, R. W. Romani, and R. Narayan. Arrival-time analysis for a millisecond pulsar. *Journal of Astrophysics and Astronomy*, 5:369–388, 1984.
- 48 G. Hobbs, A. Lyne, and M. Kramer. Pulsar Timing Noise. *Chinese Journal of Astronomy and Astrophysics Supplement*, 6(2):169–175, 2006.
- 49 G. Hobbs, A. G. Lyne, and M. Kramer. An analysis of the timing irregularities for 366 pulsars. *MNRAS*, 402:1027–1048, 2010.
- 50 R. M. Shannon and J. M. Cordes. Assessing the Role of Spin Noise in the Precision Timing of Millisecond Pulsars. *ApJ*, 725:1607–1619, 2010.
- 51 W. Coles, G. Hobbs, D. J. Champion, et al. Pulsar timing analysis in the presence of correlated noise. *MNRAS*, 418:561–570, 2011.
- 52 R. van Haasteren and Y. Levin. Understanding and analysing time-correlated stochastic signals in pulsar timing. *MNRAS*, 428:1147–1159, 2013.
- 53 P. B. Demorest, R. D. Ferdman, M. E. Gonzalez, et al. Limits on the Stochastic Gravitational Wave Background from the North American Nanohertz Observatory for Gravitational Waves. *ApJ*, 762:94, 2013.
- 54 M. J. Keith, W. Coles, R. M. Shannon, et al. Measurement and correction of variations in interstellar dispersion in high-precision pulsar timing. *MNRAS*, 429:2161–2174, 2013.
- 55 K. J. Lee, C. G. Bassa, G. H. Janssen, et al. Model-based asymptotically optimal dispersion measure correction for pulsar timing. *MNRAS*, 441:2831–2844, 2014.
- 56 X. P. You, G. Hobbs, W. A. Coles, et al. Dispersion measure variations and their effect on precision pulsar timing. *MNRAS*, 378:493–506, 2007.
- 57 R. Narayan. The Physics of Pulsar Scintillation. *Royal Society of London Philosophical Transactions Series A*, 341:151–165, 1992.
- 58 D. Stinebring. Effects of the interstellar medium on detection of low-frequency gravitational waves. *Class. Quantum Gravity*, 30(22):224006, 2013.
- 59 J. M. Cordes and R. M. Shannon. A Measurement Model for Preci-

- sion Pulsar Timing. *arXiv:1010.3785v1*, 2010.
- 60 P. B. Demorest. Cyclic spectral analysis of radio pulsars. *MNRAS*, 416:2821–2826, 2011.
  - 61 K. Liu, G. Desvignes, I. Cognard, et al. Measuring pulse times of arrival from broad-band pulsar observations. *MNRAS*, 443:3752–3760, 2014.
  - 62 J. M. Cordes, R. M. Shannon, and D. R. Stinebring. Frequency-Dependent Dispersion Measures and Implications for Pulsar Timing. *arXiv:1503.08491v1*, 2015.
  - 63 G. Hobbs, W. Coles, R. N. Manchester, et al. Development of a pulsar-based time-scale. *MNRAS*, 427:2780–2787, 2012.
  - 64 D. J. Champion, G. B. Hobbs, R. N. Manchester, et al. Measuring the Mass of Solar System Planets Using Pulsar Timing. *ApJ*, 720:L201–L205, 2010.
  - 65 F. A. Jenet, A. Lommen, S. L. Larson, et al. Constraining the Properties of Supermassive Black Hole Systems Using Pulsar Timing: Application to 3C 66B. *ApJ*, 606:799–803, 2004.
  - 66 S. Yi, B. W. Stappers, S. A. Sanidas, et al. Limits on the strength of individual gravitational wave sources using high-cadence observations of PSR B1937+21. *MNRAS*, 445:1245–1252, 2014.
  - 67 X. Deng and L. S. Finn. Pulsar timing array observations of gravitational wave source timing parallax. *MNRAS*, 414:50–58, 2011.
  - 68 H. Wahlquist. The Doppler response to gravitational waves from a binary star source. *General Relativity and Gravitation*, 19:1101–1113, 1987.
  - 69 S. A. Sanidas, R. A. Battye, and B. W. Stappers. Constraints on cosmic string tension imposed by the limit on the stochastic gravitational wave background from the European Pulsar Timing Array. *Phys. Rev. D*, 85(12):122003, 2012.
  - 70 W. Zhao, Y. Zhang, X.-P. You, et al. Constraints of relic gravitational waves by pulsar timing arrays: Forecasts for the FAST and SKA projects. *Phys. Rev. D*, 87(12):124012, 2013.
  - 71 M. L. Tong, Y. Zhang, W. Zhao, et al. Using pulsar timing arrays and the quantum normalization condition to constrain relic gravitational waves. *Class. Quantum Gravity*, 31(3):035001, 2014.
  - 72 M. Rajagopal and R. W. Romani. Ultra-Low-Frequency Gravitational Radiation from Massive Black Hole Binaries. *ApJ*, 446:543, 1995.
  - 73 A. H. Jaffe and D. C. Backer. Gravitational Waves Probe the Coalescence Rate of Massive Black Hole Binaries. *ApJ*, 583:616–631, 2003.
  - 74 J. S. B. Wyithe and A. Loeb. Low-Frequency Gravitational Waves from Massive Black Hole Binaries: Predictions for LISA and Pulsar Timing Arrays. *ApJ*, 590:691–706, 2003.
  - 75 Z. L. Wen, F. S. Liu, and J. L. Han. Mergers of Luminous Early-Type Galaxies in the Local Universe and Gravitational Wave Background. *ApJ*, 692:511–521, 2009.
  - 76 A. Sesana. Systematic investigation of the expected gravitational wave signal from supermassive black hole binaries in the pulsar timing band. *MNRAS*, 433:L1–L5, 2013.
  - 77 V. Ravi, J. S. B. Wyithe, G. Hobbs, et al. Does a “Stochastic” Background of Gravitational Waves Exist in the Pulsar Timing Band? *ApJ*, 761:84, 2012.
  - 78 S. T. McWilliams, J. P. Ostriker, and F. Pretorius. Gravitational Waves and Stalled Satellites from Massive Galaxy Mergers at  $z \leq 1$ . *ApJ*, 789:156, 2014.
  - 79 M. Enoki and M. Nagashima. The Effect of Orbital Eccentricity on Gravitational Wave Background Radiation from Supermassive Black Hole Binaries. *Progress of Theoretical Physics*, 117:241–256, 2007.
  - 80 A. Sesana. Insights into the astrophysics of supermassive black hole binaries from pulsar timing observations. *Class. Quantum Gravity*, 30(22):224014, 2013.
  - 81 V. Ravi, J. S. B. Wyithe, R. M. Shannon, et al. Binary supermassive black hole environments diminish the gravitational wave signal in the pulsar timing band. *MNRAS*, 442:56–68, 2014.
  - 82 F. A. Jenet, G. B. Hobbs, K. J. Lee, et al. Detecting the Stochastic Gravitational Wave Background Using Pulsar Timing. *ApJ*, 625:L123–L126, 2005.
  - 83 F. A. Jenet, G. B. Hobbs, W. van Straten, et al. Upper Bounds on the Low-Frequency Stochastic Gravitational Wave Background from Pulsar Timing Observations: Current Limits and Future Prospects. *ApJ*, 653:1571–1576, 2006.
  - 84 D. R. B. Yardley, W. A. Coles, G. B. Hobbs, et al. On detection of the stochastic gravitational-wave background using the Parkes pulsar timing array. *MNRAS*, 414:1777–1787, 2011.
  - 85 R. van Haasteren, Y. Levin, G. H. Janssen, et al. Placing limits on the stochastic gravitational-wave background using European Pulsar Timing Array data. *MNRAS*, 414:3117–3128, 2011.
  - 86 L. Lentati, S. R. Taylor, C. M. F. Mingarelli, et al. European Pulsar Timing Array limits on an isotropic stochastic gravitational-wave background. *MNRAS*, 453:2576–2598, 2015.
  - 87 R. M. Shannon, V. Ravi, W. A. Coles, et al. Gravitational-wave limits from pulsar timing constrain supermassive black hole evolution. *Science*, 342:334–337, 2013.
  - 88 V. Springel, S. D. M. White, A. Jenkins, et al. Simulations of the formation, evolution and clustering of galaxies and quasars. *Nature*, 435:629–636, 2005.
  - 89 M. Boylan-Kolchin, V. Springel, S. D. M. White, et al. Resolving cosmic structure formation with the Millennium-II Simulation. *MNRAS*, 398:1150–1164, 2009.
  - 90 A. Küllier, J. P. Ostriker, P. Natarajan, et al. Understanding Black Hole Mass Assembly via Accretion and Mergers at Late Times in Cosmological Simulations. *ApJ*, 799:178, 2015.
  - 91 N. J. Cornish and A. Sesana. Pulsar timing array analysis for black hole backgrounds. *Class. Quantum Gravity*, 30(22):224005, 2013.
  - 92 C. M. F. Mingarelli, T. Sidery, I. Mandel, et al. Characterizing gravitational wave stochastic background anisotropy with pulsar timing arrays. *Phys. Rev. D*, 88(6):062005, 2013.
  - 93 S. R. Taylor and J. R. Gair. Searching for anisotropic gravitational-wave backgrounds using pulsar timing arrays. *Phys. Rev. D*, 88(8):084001, 2013.
  - 94 J. Gair, J. D. Romano, S. Taylor, et al. Mapping gravitational-wave backgrounds using methods from CMB analysis: Application to pulsar timing arrays. *Phys. Rev. D*, 90(8):082001, 2014.
  - 95 S. R. Taylor, C. M. F. Mingarelli, J. R. Gair, et al. Limits on Anisotropy in the Nanohertz Stochastic Gravitational Wave Background. *Phys. Rev. Lett.*, 115(4):041101, 2015.
  - 96 K. S. Thorne. in *Hawking S., Israel W., eds, Three Hundred Years of Gravitation*. Cambridge Uni. Press, Cambridge, 1987.
  - 97 H. Sudou, S. Iguchi, Y. Murata, et al. Orbital Motion in the Radio Galaxy 3C 66B: Evidence for a Supermassive Black Hole Binary. *Science*, 300:1263–1265, 2003.
  - 98 A. Sesana, A. Vecchio, and M. Volonteri. Gravitational waves from resolvable massive black hole binary systems and observations with Pulsar Timing Arrays. *MNRAS*, 394:2255–2265, 2009.
  - 99 K. J. Lee, N. Wex, M. Kramer, et al. Gravitational wave astronomy of single sources with a pulsar timing array. *MNRAS*, 414:3251–3264, 2011.
  - 100 C. M. F. Mingarelli, K. Grover, T. Sidery, et al. Observing the Dynamics of Supermassive Black Hole Binaries with Pulsar Timing Arrays. *Physical Review Letters*, 109(8):081104, 2012.
  - 101 V. Ravi, J. S. B. Wyithe, R. M. Shannon, et al. Prospects for gravitational-wave detection and supermassive black hole astrophysics with pulsar timing arrays. *MNRAS*, 447:2772–2783, 2015.
  - 102 P. A. Rosado, A. Sesana, and J. Gair. Expected properties of the first gravitational wave signal detected with pulsar timing arrays. *MNRAS*,

- 451:2417–2433, 2015.
- 103 S. Babak and A. Sesana. Resolving multiple supermassive black hole binaries with pulsar timing arrays. *Phys. Rev. D*, 85:044034, 2012.
- 104 J. A. Ellis, X. Siemens, and J. D. E. Creighton. Optimal Strategies for Continuous Gravitational Wave Detection in Pulsar Timing Arrays. *ApJ*, 756:175, 2012.
- 105 J. A. Ellis. A Bayesian analysis pipeline for continuous GW sources in the PTA band. *Class. Quantum Gravity*, 30(22):224004, 2013.
- 106 S. Taylor, J. Ellis, and J. Gair. Accelerated Bayesian model-selection and parameter-estimation in continuous gravitational-wave searches with pulsar-timing arrays. *Phys. Rev. D*, 90(10):104028, 2014.
- 107 Y. Wang, S. D. Mohanty, and F. A. Jenet. A Coherent Method for the Detection and Parameter Estimation of Continuous Gravitational Wave Signals Using a Pulsar Timing Array. *ApJ*, 795:96, 2014.
- 108 X.-J. Zhu, G. Hobbs, L. Wen, et al. An all-sky search for continuous gravitational waves in the Parkes Pulsar Timing Array data set. *MNRAS*, 444:3709–3720, 2014.
- 109 X.-J. Zhu, L. Wen, G. Hobbs, et al. Detection and localization of single-source gravitational waves with pulsar timing arrays. *MNRAS*, 449:1650–1663, 2015.
- 110 D. R. B. Yardley, G. B. Hobbs, F. A. Jenet, et al. The sensitivity of the Parkes Pulsar Timing Array to individual sources of gravitational waves. *MNRAS*, 407:669–680, 2010.
- 111 J. P. W. Verbiest, M. Bailes, W. A. Coles, et al. Timing stability of millisecond pulsars and prospects for gravitational-wave detection. *MNRAS*, 400:951–968, 2009.
- 112 Z. Arzoumanian, A. Brazier, S. Burke-Spolaor, et al. Gravitational Waves from Individual Supermassive Black Hole Binaries in Circular Orbits: Limits from the North American Nanohertz Observatory for Gravitational Waves. *ApJ*, 794:141, 2014.
- 113 S. Babak, A. Petiteau, A. Sesana, et al. European Pulsar Timing Array Limits on Continuous Gravitational Waves from Individual Supermassive Black Hole Binaries. *arXiv:1509.02165v1*, 2015.
- 114 V. B. Braginskii and K. S. Thorne. Gravitational-wave bursts with memory and experimental prospects. *Nature*, 327:123–125, 1987.
- 115 M. Favata. Post-Newtonian corrections to the gravitational-wave memory for quasicircular, inspiralling compact binaries. *Phys. Rev. D*, 80(2):024002, 2009.
- 116 N. Seto. Search for memory and inspiral gravitational waves from supermassive binary black holes with pulsar timing arrays. *MNRAS*, 400:L38–L42, 2009.
- 117 R. van Haasteren and Y. Levin. Gravitational-wave memory and pulsar timing arrays. *MNRAS*, 401:2372–2378, 2010.
- 118 M. S. Pshirkov, D. Baskaran, and K. A. Postnov. Observing gravitational wave bursts in pulsar timing measurements. *MNRAS*, 402:417–423, 2010.
- 119 D. R. Madison, J. M. Cordes, and S. Chatterjee. Assessing Pulsar Timing Array Sensitivity to Gravitational Wave Bursts with Memory. *ApJ*, 788:141, 2014.
- 120 J. M. Cordes and F. A. Jenet. Detecting Gravitational Wave Memory with Pulsar Timing. *ApJ*, 752:54, 2012.
- 121 J. B. Wang, G. Hobbs, W. Coles, et al. Searching for gravitational wave memory bursts with the Parkes Pulsar Timing Array. *MNRAS*, 446:1657–1671, 2015.
- 122 Z. Arzoumanian, A. Brazier, S. Burke-Spolaor, et al. NANOGrav Constraints on Gravitational Wave Bursts with Memory. *arXiv:1501.05343v1*, 2015.
- 123 L. S. Finn and A. N. Lommen. Detection, Localization, and Characterization of Gravitational Wave Bursts in a Pulsar Timing Array. *ApJ*, 718:1400–1415, 2010.
- 124 A. Vilenkin. Gravitational radiation from cosmic strings. *Physics Letters B*, 107:47–50, 1981.
- 125 T. Damour and A. Vilenkin. Gravitational Wave Bursts from Cosmic Strings. *Physical Review Letters*, 85:3761, 2000.
- 126 X. Siemens, J. Creighton, I. Maor, et al. Gravitational wave bursts from cosmic (super)strings: Quantitative analysis and constraints. *Phys. Rev. D*, 73(10):105001, 2006.
- 127 P. Amaro-Seoane, A. Sesana, L. Hoffman, et al. Triplets of supermassive black holes: astrophysics, gravitational waves and detection. *MNRAS*, 402:2308–2320, 2010.
- 128 X. Deng. Searching for gravitational wave bursts via Bayesian non-parametric data analysis with pulsar timing arrays. *Phys. Rev. D*, 90(2):024020, 2014.